Numerical Simulations of Highly Efficient Cu_2FeSnS_4 (CFTS) Based Solar Cells

Fransisco Kouadio Konan*‡, Hervé Joël Tchognia Nkuissi**, Bouchaib Hartiti ***

*Laboratory of Solar Energy and Nanotechnology, Research Institute on New Energies, Nangui Abrogoua University, 02 P.O.Box 801 Abidjan, Côte d'Ivoire.
**Department of Physics, Faculty of Science, University of Yaoundé I, P.O Box 812, Yaoundé, Cameroon

***ERDyS Laboratory, Materials, Energy, Water, Modeling and Sustainable Development Group, Faculty of Science and Technique, Hassan II University of Casablanca, P.O. Box 146, 20800 Mohammedia, Morocco
(kfransisco@gmail.com, hervetchognia@gmail.com, bhartiti@gmail.com)

‡Corresponding Author; Fransisco Kouadio Konan, Research Institute on New Energies, Nangui Abrogoua University, 02 P.O.Box 801 Abidjan, Côte d'Ivoire, Tel: +225 499 49434,
Fax: +225 027 37343, kfransisco@gmail.com

Received: 01.08.2019 Accepted:16.10.2019

Abstract-Cu_2FeSnS_4 (CFTS) is like its counterpart Cu_2ZnSnS_4 (CZTS) a non-toxic and earth abundant material, with a stannite structure. It is a promising material and mainly suitable for the fabrication of low-cost and highly efficient thin film solar cells. In this work, solar cell characteristics using CFTS as the absorber material have been analyzed by numerical simulations. The influence of structural and physical parameters such as the thickness of the absorber layer, acceptor carriers concentrations densities in the absorber layer, as well as effects of back contact metal work function and operating temperature on electrical output parameters of CFTS solar cell have been evaluated by using one dimensional numerical simulation program SCAPS. Simulations results revealed that too large thicknesses affect the fill factor even if they improve slightly the other parameters. We found that it is not necessary to go beyond a thickness of 3 μm in order to make a tradeoff between the efficiency and the cost. Moreover, it is important to control the carrier density in the absorber for highly efficient CFTS solar cell. By raising the operating temperature, the cell performances are found to be affected. Numerical simulations showed optimized and promising results with the power conversion efficiency (PCE) of 22.27%, fill factor (FF) of 86.54%, short-circuit current density (J_{SC}) of 24.92 mA/cm^2 and open circuit voltage (V_{OC}) of 1.033 V. These results are interesting and therefore can define right guidelines and feasible baselines for the design and the fabrication of low-cost and highly efficient CFTS solar cells.

Keywords: Cu_2FeSnS_4, solar cell, numerical simulation, SCAPS-1D, efficiency improvement, electrical parameters

1. Introduction

Currently, intensive research is being conducted to develop solar cells made from abundant and environmentally friendly materials to compete and even replace solar cells such as high-efficiency CIGS and CdTe, but which use rare and toxic elements such as indium (In), gallium (Ga), tellurium (Te) and cadmium (Cd) [1, 2]. The quaternary chalcogenides of the Cu_2-II-IV-IV_4 family (II = Zn, Cd, IV = Sn, Ge, IV_4 = S, Se), including Cu_2ZnSnS_4 (CZTS) and $Cu_2ZnSnSe_4$ (CZTSe) have been extensively studied as promising and alternative absorber material to CIGS, thanks to their high absorption coefficient (~ 10^4 cm^{-1}) in the visible range of the solar spectrum, their optimal gap energy (1.5 eV for CZTS and 1.1 eV for CZTSe) and also the ecological nature and abundance in the earth's crust of the constituent elements [2-4]. Solar cells based on CZTS and CZTSe have so far shown a better PCE of 8.4% and 12.6%, respectively [5, 6].

The mineral material Cu_2FeSnS_4 (CFTS) of stannite structure [7], which is related to the CZTS quaternary semiconductor, can serve as a viable alternative absorber material due to its suitable gap energy (1.2-1.5 eV) [8-12], its abundant and non toxic constituents [2], and its high absorption coefficient (> 10^4 cm^{-1}) [13-18]. CFTS-based solar cells have already been fabricated in the laboratory and showed PCEs of 2.73% [15] and 0.29% [19]. The PCE of these solar cells needs to be improved, by studying deeply the

synthesis and manufacturing mechanisms as well as understanding the operating modes and performances of this type of solar cell.

Numerical simulation is an effective and necessary tool to achieve such a goal because it allows evaluating the theoretical concepts on the optical and electrical characteristics of a solar cell as well as its performances. It also allows a good understanding of the operating parameters of a photovoltaic device and plays a key role in the design and manufacture of the solar cell itself. In this study, the FTO/TiO_2/CFTS/back metal contact solar cell was simulated and analyzed. The effects of several structural and physical parameters of the cell on its electrical characteristics have been studied. The results obtained can serve as a basis for the design and manufacture of high efficiency CFTS solar cells. The one-dimensional simulation program Solar Cell Capacitance Simulator (SCAPS) has been used in this work and the details of the structure and simulation procedure of the cell are presented in the following sections.

1. Simulation program and structure of the solar cell

1.1 Simulation program

In this study, the numerical simulation of the CFTS solar cell was carried out by the one-dimensional solar simulator SCAPS. The structural and physical parameters of each layer of the cell are incorporated into the simulator as input parameters to the simulation. Written and maintained by Marc Burgelman and his colleagues in the Department of Electronics and Information Systems (ELIS) at the University of Gent in Belgium, it was designed for the simulation of polycrystalline heterojunction solar cells [20]. Initially, it was used and tested with the solar cells of the $CuInSe_2$ and CdTe family of materials; and since then, several extensions have improved its possibilities to take into account other structures including thin films [21, 22]. The SCAPS simulator is able to simulate up to 7 layers, in addition to two layers of the front and the back contacts. All the physical and optoelectronic properties of each layer can be displayed and modified in a separate window [23]. It is therefore possible to simulate a number of common measurements such as the I-V, C-V and C-*f* characteristics at equilibrium and under illumination and the quantum efficiency QE. Moreover, important information such as energy band diagram, generation and recombination profiles, electric field distributions, charge carrier densities etc. can also be extracted from a simulation by SCAPS [20, 24]. All this information is computed by SCAPS on the basis of the Poisson's equation and the continuity equation of free electrons and free holes and given respectively by the following expressions [23]:

$$\frac{\partial}{\partial x}\left(\varepsilon_0 \varepsilon \frac{\partial \psi}{\partial x}\right) = -q\left(p - n + N_D^+ - N_A^- + \frac{\rho_{def}}{q}\right) \quad (1)$$

$$-\frac{\partial J_n}{\partial x} - U_n + G = 0 \quad (2)$$

$$-\frac{\partial J_p}{\partial x} - U_p + G = 0 \quad (3)$$

where ψ is the electrostatic potential, n and p free electron and free hole, N_D^+ and N_A^- the concentrations of the ionized donor and the ionized acceptor. J_n and J_p are the respective current densities of electrons and holes. The term G is the optical generation rate of the charge carriers and U their recombination rate.

1.2 Solar cell structure and simulation parameters

The basic structure used for our simulations is essentially composed of a FTO window layer, a TiO_2 electron transport layer (buffer layer), a CFTS absorber layer and Molybdenum back contact layer. Fig. 1 illustrates in a simple way the schematic structure of the solar cell used in this work. The cell was illuminated from the front FTO surface to the back with the default AM 1.5G illumination spectrum for all simulations. The default operating temperature has been fixed at 300 K. The main physical and optoelectronic parameters used in our simulations are listed in Table 1. These parameters were chosen from literature, theory or in some cases objectively estimated [15, 25-28].

2. Results et discussion

2.1 Basic CFTS-based solar cell simulation

The main function of a solar cell is to convert solar radiation into electricity. In the absence of light, the solar cell behaves like a large flat diode [28]. A solar cell starts working in the presence of light; the generation of charge carriers due to the absorption of photons from the incident radiation is the main reason for the flow of current. In this work, the SCAPS-1D simulation program was used to evaluate and record the electrical output parameters of the FTO/TiO_2/CFTS/Mo solar cell. The curves of the J-V characteristics as well as the quantum efficiency under illumination resulting from the simulation using the values of Table 1 are shown in Fig. 2.

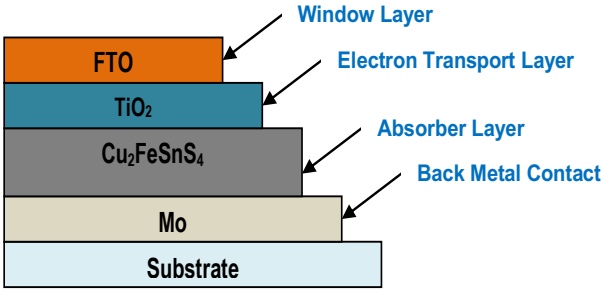

Fig. 1. CFTS solar cell structure used in this work

Table 1. Parameters used in our simulations

Parameters	Window Layer	Buffer Layer	Absorber Layer

Material	FTO	TiO_2	CFTS
Thickness (µm)	0.3	0.04	2
Band gap energy (eV)	3.5	3.2	1.36
Electron affinity (eV)	4	3.86	3.3
Dielectric permittivity (relative)	9	9	9
CB effective density of states (cm^{-3})	1×10^{18}	1.8×10^{18}	2.2×10^{18}
VB effective density of states (cm^{-3})	1×10^{19}	2.4×10^{19}	1.8×10^{19}
Electron thermal velocity (cm/s)	1×10^{7}	1×10^{7}	1×10^{7}
Hole thermal velocity (cm/s)	1×10^{7}	1×10^{7}	1×10^{7}
Electron mobility (cm^2/Vs)	20	100	2×10^{1}
Hole mobility (cm^2/Vs)	10	25	2.2×10^{1}
Donor density N_D (cm^{-3})	1×10^{18}	1×10^{15}	0
Acceptor density N_A (cm^{-3})	0	0	2×10^{18}
Absorption coefficient	1×10^{1}	1×10^{1}	5×10^{4}

The calculated output electrical parameters are shown in Fig. 2 (a). The simulated solar cell showed a conversion efficiency of 20.44%. As can be seen in Fig. 2 (b), almost 80% of photons in the visible range of solar radiation are absorbed by the material. The drop in the quantum efficiency curve around 900 nm corresponds to the CFTS band gap energy [29-31]. There is also low recombination losses on the FTO surface as can be seen in Fig. 2 (b). The electrical parameters of a solar cell such as open-circuit voltage (Voc) and short-circuit current density (Jsc), in addition to quantum efficiency and series resistances are fundamental factors that can limit performance of the solar cell [32]. These parameters must be constantly controlled in order to improve and maintain the performance of these solar cells.

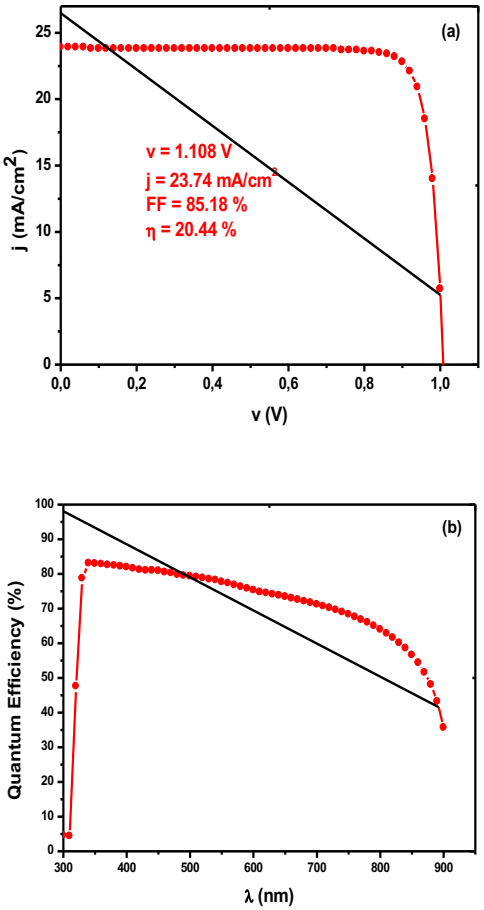

Fig. 2. Curves: (a) J-V characteristics and (b) Quantum efficiency of the simulated CFTS-based solar cell

3.2 Effect of CFTS absorber layer thickness

The effect of the CFTS absorber layer thickness was evaluated by varying its value from 1µm to 10µm, while keeping the other parameters of the entire cell constants. Fig. 3 shows the effect of CFTS thickness on electrical parameters of the whole cell. It is observed that the values of the open circuit voltage (Voc), the short circuit current density (Jsc) and the PCE (η) increase with the increase in the thickness of the CFTS and start to stabilize above 3µm. The fill factor (FF) meanwhile, after reaching the value of 2µm, decreases. The increase in values of Voc, Jsc and PCE up to an optimal value of CFTS thickness is mainly due to the absorption of more photons with longer wavelengths, which in turn affects the ratio of photo-generated carriers; this explains the decrease of the fill factor (FF) values. The absorption of more photons with longer wavelengths will allow generating a significant number of electron-hole pairs and therefore collecting at the front contact an interesting amount of free electrons. This will improve the values of Jsc and PCE.

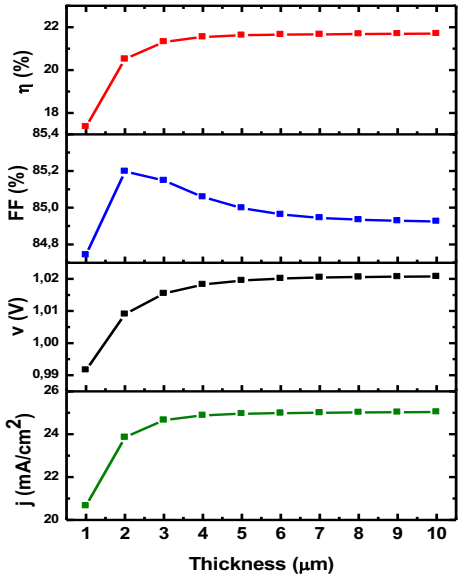

Fig. 3. Effect of the CFTS absorber layer thickness on the electrical parameters of the solar cell

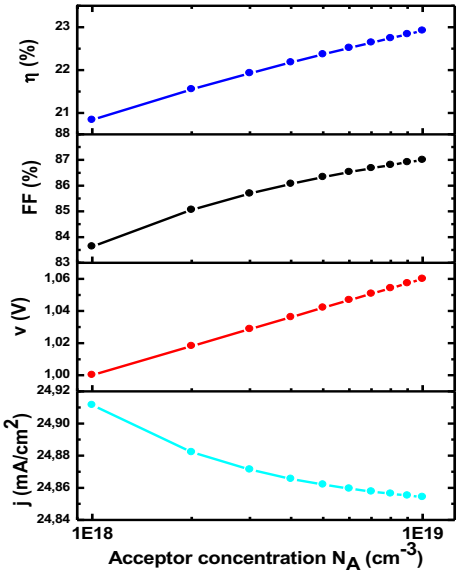

Fig. 4. Effect of acceptor concentration N_A in the CFTS absorber layer

On the other hand, the more electron-hole pairs, the more the mobility of the photo-generated carriers will be influenced and their ability to reach the front contact and to be collected will be reduced. This is the reason for the decrease in FF [33-35]. In order to avoid the ratio of the photo-generated carriers to be too much affected and also in order to find a tradeoff between the efficiency of the cell and its cost, it is not necessary to choose too large thicknesses for the absorber layer. Thus, the value of 3 µm was chosen as the optimal value of the thickness of the absorber layer by our numerical simulations.

3.3 Effect of acceptor concentration in the absorber layer

The acceptor concentration density (N_A) in the CFTS absorber layer was varied from $1x10^{18}$ cm^{-3} to $1x10^{19}$ cm^{-3} as can be seen in Fig. 4 in order to study its variations on the output parameters of the cell. Fig. 4 shows that the Voc increases with increasing concentration of doping levels while Jsc decreases when it increases. The main reason is that the saturation current of the whole cell increases as the doping concentration increases; which justifies the increase of Voc [28]. However, increasing the doping concentration increases the recombination process due to the introduction of recombination centers or traps into the layer. This recombination process reduces the ability of the photo-generated carriers to be collected at the front; hence the drop in the values of Jsc [36]. It can be seen that the probability of collection strongly depends on the influence of the doping concentration. As the doping concentration in the CFTS layer increases, the semiconductor becomes degenerate and this is a valid and necessary condition for limiting the N_A value [37]. It is also seen in Fig. 4 that the fill factor and PCE increase with the increase in doping concentration in the absorber layer due certainly to the increase in Voc. Therefore, we can use the value $3x10^{18}$ cm^{-3} as the optimal value given by our simulations.

3.4 Effect of back metal contact work function

The back metal contact work function can also affect the overall performance of a solar cell. The effect of this characteristic on the electrical output parameters of the cell has also been explored and the results of such a study are presented in Fig. 5. To evaluate the effects of the back metal contact work function, its value has been varied from 4.5 eV to 5.5 eV. An improvement in the output parameters of the simulated solar cell is observed when the back metal contact work function increases as can be seen in Fig. 5. It is also seen that all parameters are unchanged between 4.5 eV and 4.7 eV, raising substantially from 4.7 to 4.9 eV and stabilizing beyond that.

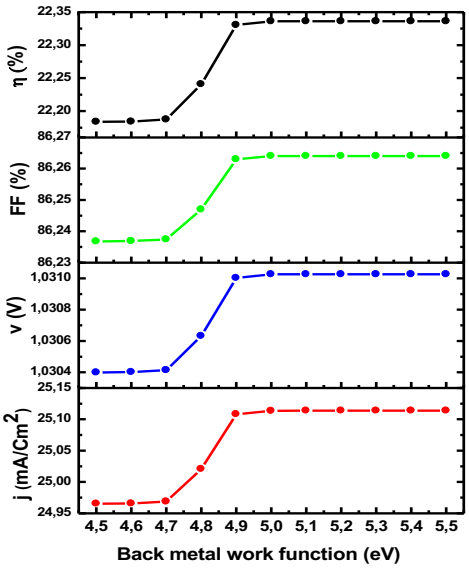

Fig. 5. Effect of back metal contact work function on electrical output parameters of the solar cell

The increase in the back metal contact work function is due to the increase of the Schottky barrier created at the back contact, which limits strong recombination of charge carriers [38]. This phenomenon can improve the value of the Voc and therefore the PCE. The optimal value for the back metal contact work function given by our simulations is therefore 4.9 eV.

3.5 Effect of operating temperature on solar cell performances

Since the solar cell is exposed to the sun constantly, it is important to study its behavior according to its operating temperature in order to evaluate its performance. Increasing the temperature of the radiation can strongly affect the performance of a solar cell [39]. Since the solar cell generally operates at temperatures above 300 K, we have evaluated the effect of this temperature on the electrical output parameters by varying it from 300 K to 600 K. The results of this study are presented in Fig. 6 below. It is observed in Fig. 6 that the values of Voc, FF and PCE decrease sharply with increasing operating temperature while Jsc increases slightly when it increases. At high temperatures, carrier concentration, gap energy, electron mobility and hole mobility are affected and this is the reason for the decrease in PCE [11, 40]. As the temperature increases, the electrons in the cell gain more energy, which makes them more unstable and more likely to recombine before reaching the space charge region [37]. Such a phenomenon contributes to decrease the values of Voc and FF [41]. The value of 300 K is therefore the optimum value for the operating temperature of the solar cell given by our simulations.

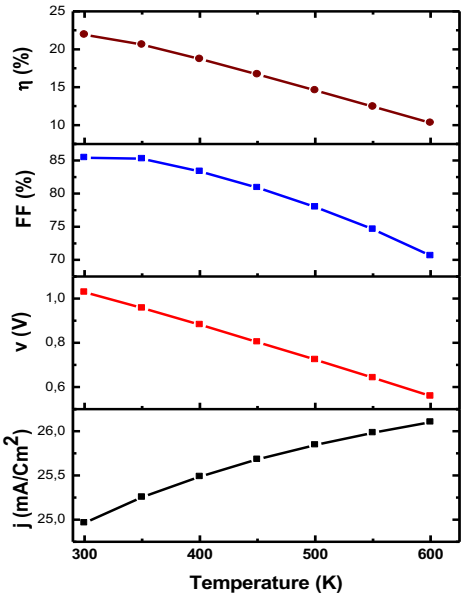

Fig. 6. Effect of the operating temperature on output parameters of the simulated solar cell

In order to simulate the optimized solar cell, the optimal values of the parameters whose effects on the electrical characteristics of the cell have been studied previously, have been adopted. A thickness of 3µm of the CFTS layer, a doping concentration of $3x10^{18}$ cm^{-3} in the CFTS layer, a back metal contact work function of 4.9 eV and an operating temperature of 300 K were selected as optimal values for a better performance of the CFTS cell output characteristics. Fig. 7 (a) shows the J-V characteristics of the optimized CFTS cell. A better performance of the simulated cell showed a PCE of 22.27%, a Jsc of 24.92 mA/cm^2, a Voc of 1.033 V and a FF of 86.54%. It is seen also in Fig. 7 (b) that there is a slight improvement in the absorption of photons in the optimized solar cell compared to the initial solar cell although weak recombination losses are still observed on the front surface.

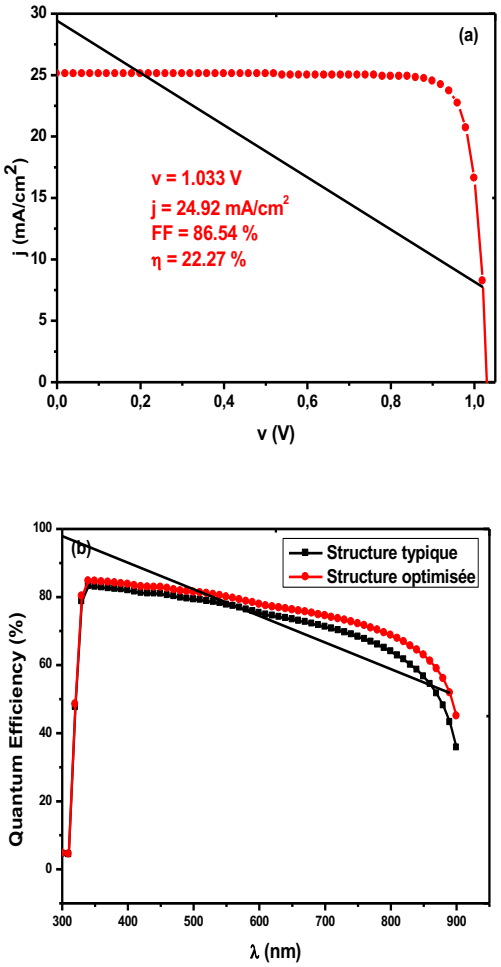

Fig. 7. Curves: (a) J-V characteristics and (b) Quantum efficiency of the optimized CFTS solar cell

3. Optimized CFTS based solar cell

4. Conclusion

The basic numerical simulation of the FTO/TiO_2/CFTS/Mo solar cell was carried out in this work using the SCAPS solar simulator. The results of our simulations have shown that the structural parameters of the layers as well as the whole cell have different effects on the electrical output characteristics of the solar cell. To better understand this type of solar cell, it is important to conduct several other simulations that can take into account various other parameters and different conditions to find the structure that will be better with this material. In this work, promising optimized results were achieved showing a PCE of 22.27%, a Jsc of 24.92 mA / cm^2, a Voc of 1.033 V and an FF of 86.54%. These results can serve as a basis and guidance for researchers and engineers not only to take a serious interest in CFTS solar cells, but also to design and manufacture them.

Acknowledgments

The authors are grateful to Dr. Marc Burgelman of the University of Gent, Belgium for producing the SCAPS simulation program.

References

[1] M. A Green, K. Emery, Y. Hishikawa, W. Warta, E. D. Dunlop, "Solar Cell Efficiency Tables (version 42)", Prog. Photovoltaics, Vol. 21, pp. 827-837, 2013.

[2] C. Waida, A. Alivisatos, D. Kammen, "Material Availability Expands the Opportunity for Large-Scale Photovoltaic Development", Environ. Sci. Technol., Vol. 43, pp. 2072-2077, 2009.

[3] H. Katagiri, K. Saitoh, T. Washio, H. Shinohara, T. Kurumasani, S. Miyajima, "Development of Thin Film Solar Cell Based on Cu_2ZnSnS_4 Thin Films", Sol. Energy Mater. Sol. Cells, Vol. 65, pp. 141-148, 2001.

[4] W. Yang, H. S. Duan, B. Bob, H. Zhou, B. Lei, C. Chung, S. Li, W. W. Hou, Y. Yang, "Novel Solution Processing of High Efficiency Earth-Abundant $Cu_2ZnSn(S,Se)_4$ Solar Cells", Adv. Mater., Vol. 24, pp. 6323-6329, 2012.

[5] B. Shin, O. Gunawan, Y. Zhu, N. A. Bojarczuk, S. J. Chey, S. Guha, "Thin film Solar Cell with 8.4% Power Conversion Efficiency Using an Earth-Abundant Cu_2ZnSnS_4 absorber", Prog. Photovoltaics, Vol. 21, pp. 72-76, 2013.

[6] W. Wang, M. T. Winkler, O. Gunawan, T. Gokmen, T. K. Todorov, Y. Zhu, D. B. Mitzi, "Device Characteristics of CZTSSe Thin Film Solar Cell With 12.6% Efficiency", Adv. Energy Mater., doi:10.1002/aenm.201301465, Vol. 4, pp. 1-5, 2014.

[7] S. R. Hall, J. T. Szymanski, J. M. Stewart, "Kesterite $Cu_2(Zn,Fe)SnS_4$ and Stannite $Cu_2(Fe,Zn)SnS_2$, Structurally Similar but Distinct Minerals", Can. Miner., Vol. 16, pp. 131-137, 1978.

[8] C. Dong, G.Y. Ashebir, J. Qi, J. Chen, Z. Wan, W. Chen, M. Wang, "Solution-processed Cu_2FeSnS_4 thin films for photovoltaic application", Mater. Lett., http://dx.doi.org/10.1016/j.matlet.2017.12.032, Vol. 214, pp. 287–289, 2018.

[9] Y. Liu, M. Hao, J. Yang, L. Jiang, C. Yan, C. Huang, D. Tang, F. Liu, Y. Liu, "Colloidal synthesis of $Cu_2FeSnSe_4$ nanocrystals for solar energy conversion", Mater. Lett., http://dx.doi.org/10.1016/j.matlet.2014.08.072, Vol. 136 pp. 306–309, 2014.

[10] X. Meng, H. Deng, J. He, L. Sun, P. Yang, J. Chu, "Synthesis, structure, optics and electrical properties of Cu_2FeSnS_4 thin film by sputtering metallic precursor combined with rapid thermal annealing sulfurization process", Mater. Lett., http://dx.doi.org/10.1016/j.matlet.2015.03.046, Vol. 151, pp. 61 – 63, 2015.

[11] X. Meng, H. Deng, J. Tao, H. Cao, X. Li, L. Sun, P. Yang, J. Chu, "Heating rate tuning in structure, morphology and electricity properties of Cu_2FeSnS_4 thin films prepared by sulfurization of metallic precursors", J. Alloys Compd., http://dx.doi.org/10.1016/j.jallcom.2016.04.166, Vol. 680, pp. 446–451, 2016.

[12] R. R. Prabhakar, N. Huu Loc, M. H. Kumar, P. P. Boix, S. Juan, R. A. John, S. K. Batabyal, L. H. Wong, "Facile water-based spray pyrolysis of earth-abundant Cu_2FeSnS_4 thin films as an efficient counter electrode in dye-sensitized solar cells", http://dx.doi.org/10.1021/am503888v, ACS Appl. Mater. Interfaces, Vol.6, pp. 17661–17667, 2014.

[13] X. Zhang, N. Bao, K. Ramasamy, Y.-H. A. Wang, Y. Wang, B. Lin, A. Gupta, "Crystal phase-controlled Synthesis of Cu_2FeSnS_4 nanocrystals with a band gap of around 1.5eV", Chem.Commun., http://dx.doi.org/10.1039/c2cc31648j, Vol. 48, pp. 4956- 4958, 2012.

[14] P. Nazari, A. Yazdani, Z. Shadrokh, B. A. Nejand, N. Farahani, R. Sei, "Band gap engineering of $Cu_3FexS_{(1-x)}S_4$: a potential absorber material for solar energy", J. Phys. Chem. Solids, http://dx.doi.org/10.1016/j.jpcs.2017.07.005, Vol. 111, pp. 110–114, 2017.

[15] D. B. Khadka, J. Kim, "Structural transition and band gap tuning of $Cu_2(Zn,Fe)SnS_4$ chalcogenide for photovoltaic application", J. Phys. Chem. *C*, http://dx.doi.org/10.1021/jp503678h, Vol. 118, pp. 14227–14237, 2014.

[16] H. Guan, H. Shen, B. Jiao, X. Wang, "Structural and optical properties of Cu_2FeSnS_4 thin film synthesized via a simple chemical method", Mater.Sci.Semicond.Process., http://dx.doi.org/10.1016/j.mssp.2013.10.021, Vol. 25, pp. 159–162, 2014.

[17] M. Adelifard, "Preparation and characterization of Cu_2FeSnS_4 quaternary semiconductor thin films via the spray pyrolysis technique for photovoltaic applications", J. Anal. Appl. Pyrolysis, http://dx.doi.org/10.1016/j.jaap.2016.09.022, Vol. 122, pp. 209–215, 2016.

[18] X. Jiang, W. Xu, R. Tan, W. Song, J. Chen, "Solvothermal synthesis of highly crystallized quaternary chalcogenide Cu_2FeSnS_4 particles", Mater. Lett., http://dx.doi.org/10.1016/j.matlet.2013.03.102, Vol. 102–103, pp. 39–42, 2013.

[19] C. Dong, W. Meng, J. Qi, M. Wang, ", Cu_2FeSnS_4 nanocrystals as effective electron acceptors for hybrid solar cells", Mater. Lett., http://dx.doi.org/10.1016/j.matlet.2016.11.090, Vol. 189, pp. 104–106, 2017.

[20] M. Burgelman, P. Nollet and S. Degrave, "Modelling polyristalline semiconductor solar cells", Thin Solid Films, Vol. 362-361, pp. 527-532, 2000.

[21] A. Niemegeers and M. Burgelman, "Effects of the Au/CdTe back contact on I(V) and C(V) characteristics of Au/CdTe/CdS/TCO solar cells", J.Appl.Phys., Vol. 81, N°6, pp. 2881-2886, 1997.

[22] M. Burgelman, J. Verschraegen, S. Degrave, P. Nollet, "Modeling Thin-film PV Devices", Progress in Photolvaics: Research and Applications, Vol. 12, pp. 143-153, 2004.

[23] M. Burgelman, K. Decok, A. Niemegers, J. Verschraegen, S. Degrave, "SCAPS manual, version: 29 December 2016".

[24] U. Mandadapu, S. Victor Vedanayakam, K. Thyagarajan, M. Raja Reddy, B. J. Babu, "Design and Simulation of High Efficiency Tin Halide Perovskite Solar Cell", International Journal Of Renewable Energy Research, Vol.7, No 4, pp. 1603-1612, December 2017.

[25] H. W. Shuo Wang, R. Ma, C. Wangb, Shina Li, "Fabrication and photoelectric properties of Cu_2FeSnS_4 (CFTS) and $Cu_2FeSn(S,Se)_4$ (CFTSSe) thin film", Appl.Surf.Sci., http://dx.doi.org/10.1016/j.apsusc.2017.05.244, Vol. 422, pp. 39-45, 2017.

[26] A. Ghosh, D. K. Chaudhary, A. Biswas, R. Thangavel, G. Udayabhanu, "Solution-processed Cu_2XSnS_4 (X=Fe, Co Ni) photo-electrochemical and thin film solar cells on vertically grown ZnO nanorod arrays", RSC Adv., http://dx.doi.org/10.1039/C6RA24149B, Vol. 6, pp. 115204–115212, 2016.

[27] H. Hou, H. Guan, L. Li, "Synthesis of Cu_2FeSnS_4 thin films with stannite and wurtzite structure directly on glass substrates via the solvothermal method", J.Mater.Sci.Mater.Electron., http://dx.doi.org/10.1007/s10854-017-6469-6, Vol. 28, pp. 7745 – 7748, 2017.

[28] Y. H. Khattak, F. Baig, S. Ullah, B. Mari, S. Beg, H. Ullah, "Numerical modeling baseline for high efficiency (Cu_2FeSnS_4) CFTS based thin film kesterite solar cell", Optik, Vol. 164, pp. 547-555, 2018.

[29] D. A. Sunter, B. Murray, M. Lehmann, R. Green, B. Ke, B. Maushund, D. M. Kammen, "Two-Stage Monte Carlo Simulation to Forecast Levelized Cost of Electricity for Wave Energy", 6th International Conference on Renewable Energy research and Applications, San Diego, pp. 638-641, Nov. 5-8, 2017.

[30] A. Bouhouta, S. Moulahoum, N. Kabache, I. Colak, « Simplicity and Performance of Direct Current Control DCC compared with other Identification Algorithms for Shunt Active Power Filter », 7th International Conference on Renewable Energy research and Applications, Paris, pp. 1352-1357, Oct. 14-17, 2018.

[31] F. M. Aboshady, M. Sumner, D. W. P. Thomas, "A Wideband Fault Location Scheme for Active Distribution Systems" 7th International Conference on Renewable Energy research and Applications, Paris, pp. 891-896, Oct. 14-17, 2018.

[32] M. Patel and A. Ray, "Enhancement of output performance of Cu thin film solar cells-A numerical simulation approach and comparison to experiments", Physica B, Vol. 407, pp. 4391–4397, 2012.

[33] M. Garba, M. T. Tankari, G. Lefebvre, "Methodology for Analyzing of a Grid Weakness and Resiliency Factors-case of Niger National Grid", 7th International Conference on Renewable Energy research and Applications, Paris, pp. 1259-1265, Oct. 14-17, 2018;

[34] M. Saleh, Y. Esa, N. Onuorah, A. A. Mohamed, "Optimal Microgrids Placement in Electric Distribution Systems Using Complex Network Framework", 6th International Conference on Renewable Energy research and Applications, San Diego, pp. 1036-1040, Nov. 5-8, 2017.

[35] D. P. Andrea, D. N. Luigi Pio, M. Santolo, « Super Twisting Sliding mode control of Smart-Inverters grid-connected for PV applications », ", 6th International Conference on Renewable Energy research and Applications, San Diego, pp. 793-796, Nov. 5-8, 2017.

[36] A. Chatterje, S. Biswas, A. Sinha, "Tunneling Current of an AlGaAs/GaAs Multiple quantum-well Solar Cell Considering a Trapezoidal Potential Barrier", International Journal Of Renewable Energy Research, Vol. 8, No 2, pp. 672-681, June 2018.

[37] J. H. Nkuissi Tchognia, B. Hartiti, J.-M. Ndjaka, Abderraouf Ridah and Philippe Thevenin, « Performances des cellules solaires à base de Cu_2ZnSnS_4 (CZTS) : Une analyse par simulations numériques via le simulateur SCAPS » *Afrique SCIENCE*, Vol. 11, N° 4, pp. 16-23, 2015.

[38] J. H. Nkuissi Tchognia, Y. Arba, K. Dakhsi, B. Hartiti, J.-M. Ndjaka, A. Ridah, P. Thevenin, "Optimization of the output parameters in kesterite-based solar cells by AMPS-1D", IEEE 2nd International Renewable and Sustainable Energy Conference (IRSEC'15), Marrakesh-Ouarzazate, pp. 1-6, 10-13 December 2015.

[39] N. Yasrebi, B. Bagheri, P. Yazdanfar, B. Rashidian, P. Sasanpour**,** "Optimization of Sputtering Parameters for the Deposition of Low Resistivity Indium Tin Oxide Thin Films"**,** Acta Metall. Sin. (Engl. Lett.), Vol. 27(2), pp. 324–330**,** 2014.

[40] N. Yasrebi, B. Bagheri, P. Yazdanfar, B. Rashidian, "Deposition of Indium-Tin-Oxide (ITO) Nanoparticles using a Sol-Electrophoretic Technique", 4th Int'l Conf. on Nanostructures (ICNS4), Kish Island, 12-14 Mar 2012.

[41] R. Kottokkaran, H. Gaonkar, B. Bagheri, V. L. Dalal, "Efficient p-i-n inorganic $CsPbI_3$ perovskite solar cell deposited using layer-by-layer vacuum deposition", Journal of Vacuum Science and Technology, May 2018.